Tubulin Assembly, Taxoid Site Binding, and Cellular Effects of the Microtubule-Stabilizing Agent Dictyostatin†

Charitha Madiraju,‡ Michael C. Edler,§ Ernest Hamel,§ Brianne S. Raccor,|| Raghavan Balachandran,‡ Guangyu Zhu,|| Kenneth A. Giuliano,⊥,# Andreas Vogt,⊥ Youseung Shin,|| Jean-Hugues Fournier,|| Yoshikazu Fukui,|| Arndt M. Brückner,|| Dennis P. Curran,|| and Billy W. Day*,‡,||

Departments of Pharmaceutical Sciences, Chemistry, and Pharmacology, University of Pittsburgh, Pittsburgh, Pennsylvania 15261, and Screening Technologies Branch, Developmental Therapeutics Program, Division of Cancer Treatment and Diagnosis, National Cancer Institute at Frederick, National Institutes of Health, Frederick, Maryland 21702

Received April 14, 2005; Revised Manuscript Received July 30, 2005

ABSTRACT: (−)-Dictyostatin is a sponge-derived, 22-member macrolactone natural product shown to cause cells to accumulate in the G2/M phase of the cell cycle, with changes in intracellular microtubules analogous to those observed with paclitaxel treatment. Dictyostatin also induces assembly of purified tubulin more rapidly than does paclitaxel, and nearly as vigorously as does dictyostatin's close structural congener, (+)-discodermolide (Isbrucker et al. (2003), *Biochem. Pharmacol. 65*, 75−82). We used synthetic (−)-dictyostatin to study its biochemical and cytological activities in greater detail. The antiproliferative activity of dictyostatin did not differ greatly from that of paclitaxel or discodermolide. Like discodermolide, dictyostatin retained antiproliferative activity against human ovarian carcinoma cells resistant to paclitaxel due to β-tubulin mutations and caused conversion of cellular soluble tubulin pools to microtubules. Detailed comparison of the abilities of dictyostatin and discodermolide to induce tubulin assembly demonstrated that the compounds had similar potencies. Dictyostatin inhibited the binding of radiolabeled discodermolide to microtubules more potently than any other compound examined, and dictyostatin and discodermolide had equivalent activity as inhibitors of the binding of both radiolabeled epothilone B and paclitaxel to microtubules. These results are consistent with the idea that the macrocyclic structure of dictyostatin represents the template for the bioactive conformation of discodermolide.

Microtubules (MTs)[1] are highly dynamic elements of the cytoskeleton that orchestrate many important events in the cell. The discovery of the mechanism of action of paclitaxel, promotion of MT assembly and stabilization against disassembly, opened new arenas in cancer chemotherapy. Biochemically, paclitaxel causes signature changes with isolated tubulin. These include a concentration-dependent increase in the turbidity of tubulin-containing solutions (due to MT assembly) and a decrease in the critical concentration of tubulin required for assembly (*1*, *2*). In cells, paclitaxel causes MT stabilization and bundling, mitotic spindle disorganization, mitotic arrest, and the induction of apoptosis. Clinical success with the taxoids paclitaxel and docetaxel in the treatment of various cancers has drawn abundant interest to MTs as a validated molecular target. Over the past decade, the search for MT stabilizers has yielded the epothilones (*3*−*6*), discodermolide (*7*, *8*), laulimalide (*9*−*11*), the eleutherobins (*12*, *13*), the sarcodictyins (*14*, *15*) and peloruside A (*16*, *17*), as well as synthetically prepared structural variants of these novel entities. Many of these agents and a few of their analogues have shown in vitro and even in vivo biological activities that appear superior in some respects to those of the taxoids.

(−)-Dictyostatin (Figure 1) is a 22-membered macrolactone with 11 stereocenters, an endocyclic *Z*,*E*-dienoate and a pendant *Z*-diene. It was first isolated from a marine sponge of the genus *Spongia* collected in the Republic of Maldives and found to be a potent antiproliferative agent of nanomolar potency (*18*). Considerable structural assignment was performed in that early work, but several questions remained as to the structure of this compound. Even with the original tentative structural assignment, it was clear that the compound had great similarities to (+)-discodermolide, another potent marine sponge cytotoxin (Figure 1) (*19*). Before the true relative and absolute stereochemistry of dictyostatin was established, we synthesized chemicals designed to be hybrid discodermolide/dictyostatin structures and evaluated them for microtubule targeting actions. One of the analogues, shown also in Figure 1, indeed caused assembly of tubulin, exhibited 50% growth inhibitory (GI_{50}) potency in the low micromolar

† Supported in part by U.S. Public Health Services Grant CA078039.
* Author to whom correspondence should be addressed. Mailing address: 721 Salk Hall, University of Pittsburgh, 3501 Terrace Street, Pittsburgh, PA 15261. Phone: 1-412-648-9706. Fax: 1-412-624-1850. E-mail: bday@pitt.edu.
‡ Department of Pharmaceutical Sciences, University of Pittsburgh.
§ National Cancer Institute.
|| Department of Chemistry, University of Pittsburgh.
⊥ Department of Pharmacology, University of Pittsburgh.
Present address: Cellumen, Inc., Pittsburgh, PA 15219.
[1] Abbreviations: MT, microtubule; GI_{50}, 50% growth inhibitory concentration; DMSO, dimethyl sulfoxide; GTP, guanosine-5′-triphosphate; ddGTP, 2′,3′-dideoxyguanosine-5′-triphosphate; FBS, fetal bovine serum; MAPs, microtubule associated proteins; GAPDH, glyceraldehyde-3-phosphate dehydrogenase; HBSS, Hanks' balanced salt solution; Mes, 2-(morpholin-4-yl)ethanesulfonic acid; FITC, fluorescein-5-isothiocyanate; MSG, monosodium glutamate.

10.1021/bi050685l CCC: $30.25
Published on Web 10/21/2005

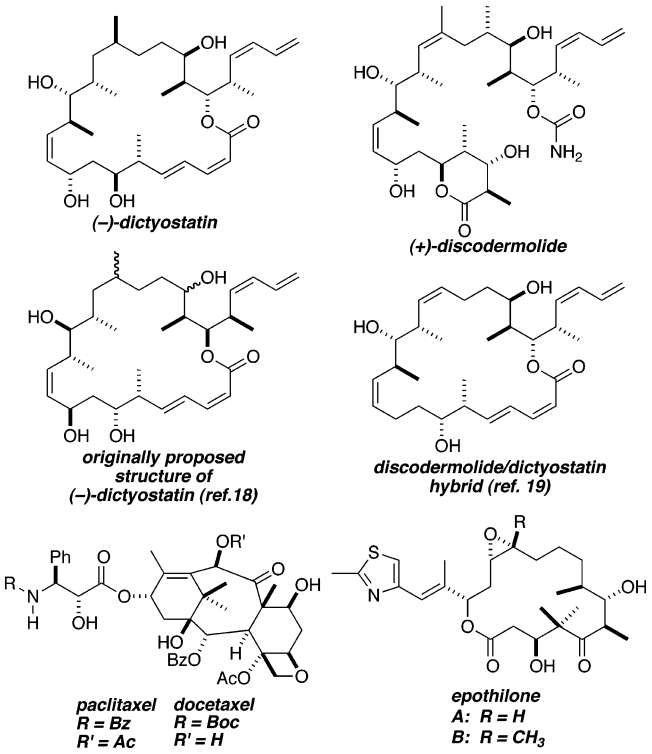

FIGURE 1: Structures of dictyostatin, discodermolide, the originally proposed structure of dictyostatin (*18*), a previously synthesized and tested discodermolide/dictyostatin hybrid molecule (*19*), paclitaxel, docetaxel, and epothilones A and B.

range (~1 μM), and competed, albeit weakly, with paclitaxel for binding to tubulin polymer (*19*).

During this time, dictyostatin was again isolated from a lithistida sponge of the family *Corallistidae* harvested near Jamaica (*20*) and shown to promote assembly of purified tubulin. The natural product was more active than paclitaxel and almost as active as discodermolide, to date the most potent of the taxoidmimetic drugs in inducing tubulin assembly (*8*, *21*). Isbrucker et al. (*20*) found dictyostatin and paclitaxel to be essentially equitoxic against several cell lines, while dictyostatin, but not paclitaxel, retained nearly full activity against two multidrug-resistant lines overexpressing the *ABC1* drug efflux transporter (P-glycoprotein). Cells treated with dictyostatin accumulated at the G2/M phase of the cell cycle and showed changes in their microtubule networks that would be expected following treatment with a taxoidmimetic compound.

A revised structure of dictyostatin was proposed based on high field NMR experiments and molecular modeling (*22*). Shortly thereafter, *de novo* syntheses of the compound gave unequivocal evidence for the structure and its absolute stereochemistry as shown in Figure 1 (*23*, *24*). These full syntheses and our previous approaches to dictyostatin/discodermolide hybrids have opened the door for the detailed biological evaluations of dictyostatin, some of which are reported here, and for synthesizing analogues of the natural product.

EXPERIMENTAL PROCEDURES

Materials

Dictyostatin was synthesized as described (*23*). Paclitaxel and [^{3}H]paclitaxel (specific activity 16.2 Ci/mmol) were provided by the Drug Synthesis and Chemistry Branch, National Cancer Institute. Discodermolide and [^{3}H]discodermolide (14.4 Ci/mmol) were generous gifts from Novartis Pharmaceuticals Corp., and epothilone B and [^{14}C]epothilone B (111 mCi/mmol) from Novartis Pharma AG. All drugs were dissolved in dimethyl sulfoxide (DMSO). Guanosine-5′-triphosphate (GTP) was obtained from Sigma and 2′,3′-dideoxyguanosine-5′-triphosphate (ddGTP) from Pharmacia; each was repurified by triethylammonium bicarbonate gradient chromatography on DEAE-Sephacel. Purified tubulin and heat-treated microtubule associate proteins (MAPs) were prepared as described previously (*25*). Tubulin freed from unbound nucleotide was prepared by gel filtration chromatography as reported earlier (*26*). Ca^{2+}- and Mg^{2+}-free RPMI-1640 culture medium were from GIBCO/BRL-Life Technologies. Fetal bovine serum (FBS) was from Hyclone. Parental human ovarian carcinoma 1A9 and the β-tubulin mutant subclone 1A9PTX10 and 1A9PTX22 cell lines were generous gifts from Drs. Tito Fojo and Paraskevi Giannakakou. Mouse anti-α-tubulin was from LabVision. Anti-glyceraldehyde-3-phosphate dehydrogenase (GAPDH) was from Biogenesis. Rabbit anti-phosphohistone H3 was from Upstate Cell Signaling, and fluorophore-labeled donkey anti-rabbit and -mouse antibodies were from Jackson Immunoresearch. All other chemicals were obtained from Sigma.

Methods

Antiproliferative Activity. Test agent-induced growth inhibition of parental (1A9) and paclitaxel-resistant (1A9PTX10 and 1A9PTX22) human ovarian adenocarcinoma cell lines was evaluated as described earlier (*27*, *28*). Cells were maintained in RPMI medium with 10% FBS. The maintenance medium of the 1A9PTX10 and 1A9PTX22 cells also contained 17 nM paclitaxel and 10 μM verapamil. Prior (48−72 h) to experimentation, resistant cells were transferred to verapamil-, paclitaxel- and phenol red-free RPMI containing 10% FBS. Cells were seeded into 96-well plates, allowed to attach and grow for 48 h, and then treated for 72 h with either DMSO (0.5% v/v; $N = 8$) or a range of concentrations, in quadruplicate, of test agents. Cell number was determined spectrophotometrically at 490 nm minus absorbance at 630 nm after exposure to 3-(4,5-dimethylthiazol-2-yl)-5-(3-carboxymethoxyphenyl)-2-(4-sulfophenyl)-2*H*-tetrazolium and *N*-methylphenazine methylsulfate. One plate for accurate determination of time zero cell numbers was always included. The fifty and one hundred percent growth inhibitory concentrations (GI_{50}, GI_{100}) of test agents were calculated from the spectrophotometrically determined growth of the control cells over the 72 h period.

Cellular Levels of Soluble and Polymerized Tubulin. Soluble and polymerized tubulin levels in cells were determined with a Western blot procedure described previously (*29*−*31*). Briefly, cells were plated in 100 mm dishes and allowed to attach for 48 h, then treated with the indicated concentrations of paclitaxel, discodermolide, or dictyostatin. After the indicated times, cells were detached by trypsinization, washed with Hanks' balanced salt solution (HBSS), then lysed in 0.1 M 2-(morpholin-4-yl)ethanesulfonic acid (Mes; pH 6.75), containing 0.1% Triton X-100, 1 mM $MgSO_4$, 2 mM EGTA, and 4 M glycerol. The lysate was centrifuged at 14 000 rpm in an Eppendorf microcentrifuge. The supernatant (soluble tubulin fraction) and pellet (polymerized

tubulin fraction) were dissolved in the in the cell lysis buffer. Protein samples were boiled in loading buffer, loaded onto 10% polyacrylamide gels, and separated by electrophoresis. Proteins were transferred to polyvinyldifluoride membranes (Biorad), using a Biorad Transblot Semidry system. After washing, blocking, and treating with appropriate antibodies, protein bands were detected using the Amersham ECL Western blotting system and Fuji film. Densitometric analyses were performed with ImageJ (v. 1.32j) software.

Multiparameter Fluorescence Microscopy. The high information content cell-based fluorescence assay was carried out under previously detailed conditions (*32*). HeLa cells growing at log phase were trypsinized and plated in 40 μL at a density of 7000−8000 cells per well in calf skin collagen I-coated 384-well plates (Falcon #3962; Fisher Scientific). Cells were exposed to test agents or 0.5% DMSO within 2−8 h of plating. Concentrated DMSO stock solutions of all test agents were diluted into solutions of HBSS medium plus 10% FBS and added to the microplate wells (10 μL per well), using an automated liquid handling system (Biomek 2000; Beckman-Coulter, Inc.) to provide a serial 2-fold dilution of each test agent. The cells were incubated in the presence of test agents for 24 h. At the end of the incubation, the medium was removed and replaced with HBSS containing 4% formaldehyde and 10 μg/mL Hoechst 33342 (25 μL/well) to fix the cells and fluorescently label their chromatin. After incubation at room temperature for 20−30 min, the solution was removed from each well and replaced with HBSS (100 μL/well). Further reagent additions were made to the microplates using the Biomek 2000. After removing the HBSS from each well, cells were permeabilized for 5 min at room temperature with 0.5% (w/w) Triton X-100 in HBSS (10 μL/well). This step extracts a fraction of the soluble cellular components, including soluble tubulin. The wells were washed with HBSS (100 μL/well), followed by addition of a primary antibody solution containing mouse anti-α-tubulin (1:3000) and rabbit anti-phosphohistone H3 (1:500) in HBSS (10 μL/well). After 1 h at room temperature, the wells were washed with HBSS as above, followed by the addition of a secondary antibody solution containing fluorescein-5-isothiocyanate (FITC)-labeled donkey anti-mouse (1:300) and Cy3-labeled donkey anti-rabbit (1:300) antibodies diluted in HBSS (10 μL/well). After 1 h at room temperature, the wells were washed as above, and HBSS was added (100 μL/well). The plates were placed in an ArrayScan HCS Reader with the Target Activation BioApplication Software coupled to Cellomics Store and the vHCS Discovery Toolbox (Cellomics, Inc.) to analyze images. Briefly, the instrument was used to scan multiple optical fields, each with multiparameter fluorescence, within a subset of the wells of the 384-well microplate. The BioApplication software produced multiple numerical feature values, such as subcellular object intensities, shapes, and location for each cell within an optical field. Data were acquired from a minimum of 1000 cells per well, except in cases where added test agents markedly reduced the attachment of cells to the substrate. A nuclear mask was generated from Hoechst 33342-stained nuclei, and object identification thresholds and shape parameters were set such that the algorithm identified over 90% of the nuclei in each field. Objects that touched each other or the edge of the image were excluded from the analysis. Tubulin mass was defined as the average green (FITC) pixel intensity in an area defined by the Hoechst-defined nuclear mask. This cytoplasmic area around the nucleus contains cytoskeletal components and has been shown to be a region from which sensitive measurements of cytoplasmic characteristics can be made (*33*). The percentage of phosphohistone H3 positive cells was defined as the number of cells whose average red (Cy3) staining intensity exceeded the average Cy3 intensity plus two standard deviations of vehicle-treated cells, divided by the total number of cells.

Tubulin Polymerization Assay. Tubulin assembly was monitored turbidimetrically at 350 nm in temperature-controlled, multichannel Gilford 250 spectrophotometers as described previously (*8*). Reaction mixtures without test compounds contained tubulin (10 μM, 1.0 mg/mL), heat-treated MAPs (0.75 mg/mL if present), GTP (100 μM if present), 4% DMSO, and 0.1 M Mes, pH 6.9. Baselines were established after addition of all reaction components except the test compounds to the cuvettes held at 0 °C. Compounds predissolved in DMSO were added to give the indicated final concentrations, and the reaction mixtures (0.25 mL final volume) were subjected to the indicated sequential temperature changes.

Electron Microscopy. Aliquots taken directly from cuvettes during turbidimetry studies were placed on 200-mesh, carbon-coated, Formvar-treated, copper grids and stained with 1% (w/v) uranyl acetate (*8*). Excess staining solution was removed by wicking with torn Whatman filter paper, and the grid was allowed to dry while protected from dust at room temperature. Grids were examined in JEOL 100CX SEM and Zeiss 10CA electron microscopes.

Tubulin Critical Concentration. The minimum concentration of tubulin necessary for each test agent at 10 μM to induce polymerization at 37 °C was determined with a centrifugation-based procedure described previously (*34*). Briefly, reaction mixtures (0.1 mL) containing varying concentrations of tubulin, 0.1 M Mes (pH 6.9), 4% DMSO, and test agents as appropriate were prepared and incubated for 30 min at 37 °C. The reaction mixtures were centrifuged for 15 min at 14 000 rpm at room temperature (20−22 °C) in an Eppendorf 5417C centrifuge. An aliquot was removed from the supernatant and its protein concentration determined by the Lowry method.

EC_{50} Determination by Centrifugation. The EC_{50} was defined as the concentration of test agent required to polymerize 50% of the tubulin compared to amount of tubulin polymer found in the pellet of the DMSO control, as described earlier (*35*). The reaction condition included 0.2 M monosodium glutamate (MSG), 10 μM tubulin, 5% DMSO and varying concentrations of test agents. The reaction mixtures were incubated at room temperature for 15 min, centrifuged for 10 min at 14 000 rpm, and protein concentration determined as above. On average 5.5 ± 4.0 (SD) % of the tubulin pelleted in the DMSO control.

Radiolabeled Ligand Binding Assays. The abilities of test agents to inhibit the binding of radiolabeled MT stabilizers from tubulin polymer were determined with a procedure described previously (*36*). [^{3}H]Paclitaxel, [^{3}H]discodermolide, and [^{14}C]epothilone B solutions were prepared as 125 μM stock solutions in 50% DMSO. Radiolabeled compound (final concentration, 4.0 μM) and test agents at final concentrations noted in the text and tables were mixed

Table 1: 50% Growth Inhibitory Concentrations (GI_{50}) of Dictyostatin, Discodermolide, and Paclitaxel against Human Ovarian Cancer Cell Lines after 72 h in Continuous Presence of the Agents as Determined by the MTS Assay[a]

	$GI_{50} \pm$ SD, nM (fold-resistance)		
test agent	1A9	1A9PTX10	1A9PTX22
dictyostatin	0.69 ± 0.80	3.2 ± 2.4 (4.6)	1.3 ± 1.0 (1.9)
discodermolide	1.7 ± 1.2	6.2 ± 3.6 (3.6)	7.0 ± 8.4 (4.1)
paclitaxel	0.71 ± 0.11	64 ± 8 (90)	51 ± 9 (72)

[a] 1A9 cells express wild-type β-tubulin, whereas the 1A9PTX10 and 1A9PTX22 cells express, respectively, the Phe270→Val and Ala364→Thr mutant forms of the protein.

in 50 μL of 4:1 (v/v) 0.75 M aqueous MSG/DMSO and warmed to 37 °C. Meanwhile, a reaction mixture containing 0.75 M MSG, 2.5 μM tubulin, and 25 μM ddGTP was prepared and incubated at 37 °C for 30 min to form MTs. A 200 μL aliquot of the MT mixture was added to the drug mixtures, and incubation continued for 30 min at 37 °C. Reaction mixtures were centrifuged in an Eppendorf 5417C centrifuge at 14 000 rpm for 20 min at room temperature. Radiolabel in the supernatants (100 μL) was determined by scintillation spectrometry. Bound radiolabeled compound was calculated from the total radiolabel added to each reaction mixture minus the amount of radiolabel found in the supernatant.

RESULTS

Inhibition of Cell Growth by Dictyostatin: Comparison with Discodermolide and Paclitaxel. Dictyostatin was evaluated in comparison with discodermolide and paclitaxel for its growth inhibitory effects on human ovarian carcinoma 1A9 cells and the two β-tubulin-mutant paclitaxel-resistant 1A9PTX10 and 1A9PTX22 cell lines (*28*). The GI_{50} values presented in Table 1 show that dictyostatin was active in the low nanomolar range and was the most potent growth inhibitory agent of the compounds studied in the paclitaxel-resistant lines. Dictyostatin and paclitaxel exhibited comparable GI_{50} values against the parental 1A9 cells (0.69 nM versus 0.71 nM), while the value obtained for discodermolide (1.7 nM) was over 2-fold higher. The mutant β-tubulin-expressing cells showed 70−90-fold resistance to paclitaxel, while their cross-resistance to dictyostatin and discodermolide was only 2−5-fold.

Soluble versus Polymerized Tubulin in Cells. The paclitaxel resistant 1A9PTX22 cells were treated for 12 h with the concentrations of dictyostatin, discodermolide, or paclitaxel that caused 50% or 100% inhibition of cell growth after 72 h (i.e., the GI_{50} and GI_{100} concentrations), or with the each of the test agents at 10 μM (and with additional higher concentrations of dictyostatin) for 4 h. The extent of cellular MT polymer was then determined by Western blot analysis. As expected (*29*), paclitaxel caused overall only a small increase in the level of polymerized tubulin in these cells. In contrast, dictyostatin or discodermolide caused increases in polymerized fraction of tubulin in the cells, an effect barely detectable even at the GI_{50} concentrations of the two agents (data not shown), but clearly evident at the GI_{100} concentrations (Figure 2A). Dictyostatin and discodermolide caused the virtually complete loss of soluble form of the protein in cells treated with micromolar concentrations of the agents (Figure 2B).

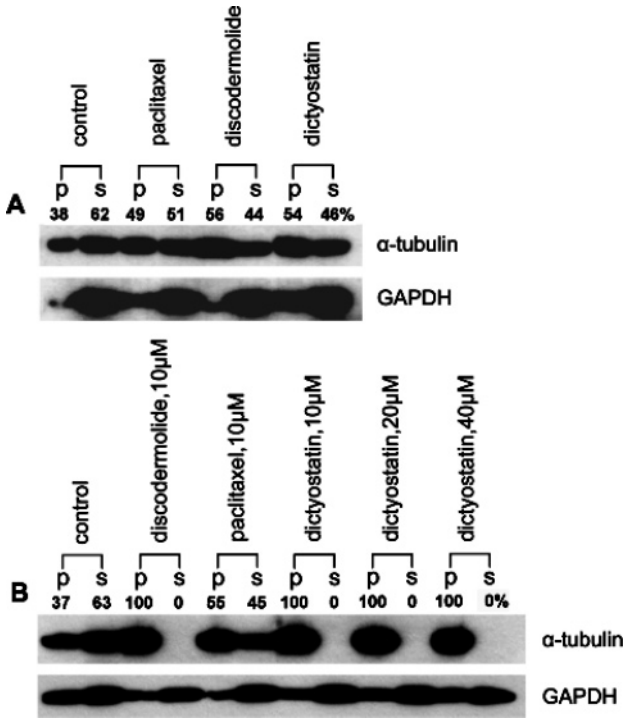

FIGURE 2: Western blot analysis of polymerized (p) and soluble (s) tubulin fractions of 1A9PTX22 cells. Panel A shows results after cells were treated for 12 h with vehicle (DMSO) or the GI_{100} concentrations of paclitaxel, 96 ($\pm$2) nM; discodermolide, 71 ($\pm$12) nM; or dictyostatin, 6.2 ($\pm$3.6) nM (standard deviations of the original determinations made with the MTS assay are shown parenthetically). Panel B shows results from cells treated for 4 h with 10 μM discodermolide, 10 μM paclitaxel, or 10, 20, or 40 μM dictyostatin. Treated cells were detached by trypsinization and washed with HBSS. The cells were then lysed in a buffer that maintained tubulin polymer but released soluble tubulin: 0.1 Mes, pH 6.75, containing 0.1% Triton X-100, 1 mM $MgSO_4$, 2 mM EGTA, and 4 M glycerol. The lysate was centrifuged, and the supernatant (soluble tubulin fraction) and pellet (polymerized tubulin fraction) were electrophoresed through denaturing 10% polyacrylamide gels. Proteins were transferred to PVDF membranes and probed with antibodies. Results of densitometric analyses are shown as the percent values for each tubulin band after normalization to total cellular GAPDH.

Multiparameter Fluorescence Analysis of Cellular Effects. The complex cellular responses that human tumor cells mounted in response to dictyostatin, discodermolide, and paclitaxel were examined with a multiplexed fluorescence cell-based assay. This assay defines the effects that test agents have on the temporal and spatial regulation of multiple cell functions and has been adopted by the pharmaceutical industry as a standard platform for compound evaluation (*37*, *38*). The multiplexed assay, which was previously validated and used to generate results for several reports (*27*, *32*, *39*, *40*), provided measurements of nuclear morphology, microtubule content, and histone H3 phosphorylation, all markers of cells at the G_2/M cell cycle boundary. HeLa cells were plated on collagen-coated 384-well microtiter plates, allowed to attach, and then treated for 24 h with dictyostatin, discodermolide, or paclitaxel at 11 concentrations over a range of more than 3 orders of magnitude, with a maximal test agent concentration of 1 μM. After the treatment period, the cells were fixed and soluble tubulin extracted with detergent. Chromatin stained with Hoechst 33342, and α-tubulin and phosphohistone H3 with primary antibodies.

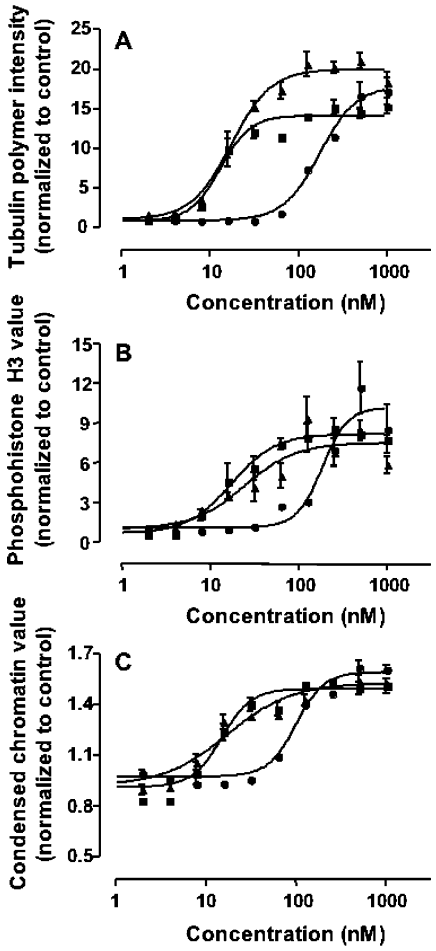

FIGURE 3: Multiparameter fluorescence analysis of the effects on HeLa cells of 24 h treatment over a range of concentrations of dictyostatin (squares), paclitaxel (triangles), and discodermolide (circles). (A) Fold-increase in the fluorescence intensity of tubulin polymer around each cell's nucleus. (B) Fold-increase in nuclear phosphohistone H3 levels. (C) Fold-increase in chromatin condensation. Cells (7000−8000 per well) were plated in calf skin collagen I-coated 384-well plates and treated with a set of serial 2-fold dilutions of each test agent for 24 h. At the end of the treatment period, cells were fixed with 4% formaldehyde and their chromatin stained with Hoechst. Cells were permeabilized with 0.5% (w/w) Triton X-100 in HBSS and treated with antibodies to α-tubulin and phosphohistone H3 for 1 h at room temperature. After an HBSS wash, FITC- and Cy3-labeled secondary antibodies were added. The plates were placed in an ArrayScan HCS Reader, a robotically controlled fluorescence microscope capable of analyzing five color ranges, with the Target Activation BioApplication Software coupled to Cellomics Store and the vHCS Discovery Toolbox (Cellomics, Inc.) to analyze individual cells in the images. Each point represents the mean ± SD of fluorescence intensity values obtained from at least 1000 cells in three independent experiments after normalization to values obtained in the control (DMSO only) cultures.

Secondary fluorophore-labeled antibodies were added and three fluorescent channels were examined on a robotically controlled fluorescence imaging system that yielded quantitative pixel distribution and density information in each channel on a per cell basis. Figure 3 shows the concentration−response curves for average tubulin polymer mass (a measure of MT stabilization), percent condensed nuclei (a measure of mitosis), and percent histone H3 phosphorylation (mitosis) in the test agent-treated cells in relationship to responses of cells treated with DMSO only. The results showed that dictyostatin and paclitaxel had nearly identical effects on all

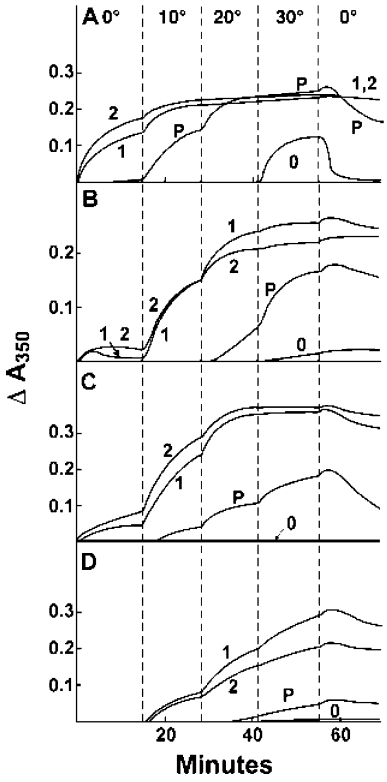

FIGURE 4: Turbidity profiles of tubulin polymerization assays, with stepwise temperature changes. Reaction mixtures contained 1.0 mg/mL (10 μM) tubulin, 0.1 M Mes (pH 6.9), 4% (v/v) DMSO, 10 μM test agent, and further additions as indicated. (A) Complete system: 0.75 mg/mL MAPs, 100 μM GTP. (B) MAPs-only system: 0.75 mg/mL MAPs. (C) GTP-only system: 100 μM GTP. (D) Tubulin-only system: no further additions. In each panel: (1) dictyostatin; (2) discodermolide; (P) paclitaxel; (0) no test agent. Reaction temperatures were as indicated, with the temperature set on the temperature controller at the time indicated by the vertical dashed line to the left of the temperature. Test agents were added to the reaction mixtures at zero time at 0 °C. Temperature in the cuvettes rose at about 0.5 °C/s and fell at about 0.1−0.15 °C/s.

three parameters in the HeLa cells. Discodermolide was about 10-fold less potent. Minimum detectable effective concentrations, determined as described previously (*27*, *32*), for increases in tubulin polymer mass with dictyostatin, paclitaxel, and discodermolide were 3.2 nM, 3.6 nM, and 40 nM, respectively; for the phosphohistone H3 response, 5.6, 6.3, and 89 nM; and for nuclear condensation, 5.0, 7.9, and 56 nM; for comparison, the 24 h GI_{50} values estimated from the cell densities determined by Hoechst staining in the multiparameter fluorescence experiments were 5.2, 4.8, and 57 nM.

Effects of Dictyostatin on Tubulin Assembly with and without MAPs and/or GTP. Tubulin assembly reactions were performed to compare 10 μM dictyostatin with 10 μM discodermolide or 10 μM paclitaxel. Test agent-induced turbidity profiles were first examined under a reaction condition in which drug is not an absolute requirement for microtubule assembly. This was the "complete system" (Figure 4A), which contained both MAPs and GTP. Because dictyostatin, like discodermolide (*8*, *21*), caused extensive assembly at 0 °C within seconds of being added to the reaction mixture, temperature was increased stepwise to 30 °C in these studies. With these two agents, temperature increases led to only small enhancements of the assembly

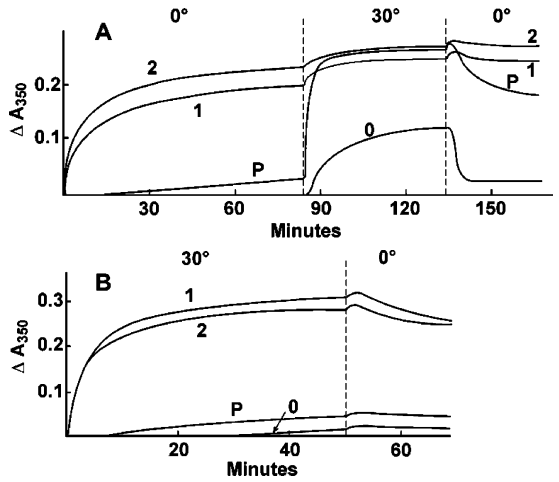

FIGURE 5: Turbidity profiles of tubulin polymerization assays, with temperature rapidly increased from 0 °C to 30 °C. Each reaction mixture contained 1.0 mg/mL (10 μM) tubulin, 0.1 M Mes (pH 6.9), 4% DMSO, 10 μM test agent, and further additions as indicated. (A) Complete system: 0.75 mg/mL MAPs, 100 μM GTP. (B) Tubulin-only system: no further additions. In each panel: (1) dictyostatin; (2) discodermolide; (P) paclitaxel; (0) no test agent. Reaction temperatures were as indicated by the vertical dashed line to the left of the temperature. See caption of Figure 4 for further details. For panel A, test agents were added to reactions at zero time at 0 °C. For panel B, test agents were added to reaction mixtures at 0 °C, and the temperature controller was set at 30 °C at zero time.

reaction, with a significant change occurring only at 10 °C. When the temperature was dropped from 30 °C back to 0 °C, the turbidity readings remained unchanged (i.e., the tubulin polymers induced by dictyostatin and discodermolide were apparently completely cold-stable). The 0 °C reaction with discodermolide was slightly more vigorous than that with dictyostatin.

With paclitaxel and as previously reported (*41*), significant assembly occurred at 10 °C but not at 0 °C, with a further increase in turbidity occurring at 20 °C. Little further change occurred at 30 °C. When the temperature was dropped to 0 °C, the paclitaxel-induced reaction mixture showed a slow, partial loss of turbidity. Previous studies (*42*) have indicated that polymer mass is about 70% cold-stable with paclitaxel following a prolonged 0 °C incubation after the assembly reaction. At 20 °C and 30 °C, the turbidity reading with paclitaxel was essentially identical with the readings obtained with dictyostatin and discodermolide.

In the absence of the test agents, polymerization only occurred at 30 °C. Extent of the reaction was much reduced as compared with the test agents. The microtubules formed at 30 °C rapidly and completely disassembled at 0 °C, as confirmed by electron microscopy.

The experiment providing results shown in Figure 5A demonstrated unequivocally the dramatic difference in the assembly promoting effects of dictyostatin and discodermolide as compared with paclitaxel at 0 °C. A prolonged incubation at 0 °C led to nearly complete polymerization with both dictyostatin and discodermolide, whereas only a minimal reaction occurred with paclitaxel. With a rapid temperature jump to 30 °C, assembly occurred much more rapidly and extensively with paclitaxel as compared with the reaction mixture without test agents. Again, similar turbidity plateaus were reached with all three test agents.

The reactions observed when either MAPs (Figure 4B) or GTP (Figure 4C) was omitted from the reaction mixture were quite similar overall. No MTs or other polymer was formed without drug in either reaction system, as confirmed by electron microscopy. The reactions with the test agents were universally shifted to higher temperatures as compared with the complete system. Thus, rapid assembly of tubulin occurred at 10 °C only with dictyostatin and discodermolide; paclitaxel required higher temperatures. The final 30 °C turbidity reading with paclitaxel was lower than with dictyostatin or discodermolide in these incomplete systems, in contrast to the complete system. When the temperature was decreased from 30 to 0 °C, there was an apparent decrease in turbidity with all test agents, except discodermolide in the MAPs only system. This has not yet been studied further.

The data shown in Figure 4 are representative of observations made in many repetitions of these experiments. Thus, the small increase and subsequent decline in turbidity observed at 0 °C with dictyostatin in the MAPs-only system (Figure 4B) indicates a subtle mechanistic difference as compared with discodermolide. It suggests a failure of polymer propagation following nucleation. Second, greater overall turbidity was observed with dictyostatin than with discodermolide in the MAPS-only system (Figure 4B), as well as with tubulin only (see below, Figure 4D). Thus, GTP appears to play a modulating role in the apparent relative activities of dictyostatin and discodermolide. Finally, with 10 μM paclitaxel, only a weak reaction was observed at 10 °C in the GTP-only system (Figure 4C) but no reaction was observed for paclitaxel at this temperature in the MAPs-only system (Figure 4B).

When both MAPs and GTP were omitted from the reaction mixture (tubulin-only system, Figure 4D), there was a further shift to higher temperatures for assembly to occur with dictyostatin or discodermolide, and only minimal turbidity development occurred with paclitaxel even at 30 °C. None of the test agents induced assembly at 0 °C. Turbidity increases were observed with dictyostatin and discodermolide at 10 °C, and each subsequent increase in temperature led to similar increases in turbidity. To obtain rapid assembly with 10 μM dictyostatin or discodermolide (but not with paclitaxel), a 0 to 30 °C temperature jump was required (Figure 5B), and with both compounds turbidity plateaus were reached within 40 min. There was a very slow decrease in turbidity with all compounds when temperature was returned to 0 °C. As noted above, under this reaction condition the turbidity plateau obtained with dictyostatin was always somewhat higher that that obtained with discodermolide. The slight turbidity increase observed without test agent probably represents tubulin denaturation. No polymer was observed under this reaction condition in the electron microscope.

Electron Microscopic Evaluation of Dictyostatin-Induced Polymer. The immunofluorescence studies of Isbrucker et al. (*20*), as well as the demonstration of mitotic arrest presented above, are consistent with the enhanced turbidity development observed with dictyostatin representing drug-induced MT assembly. Nevertheless, it was important to demonstrate this by electron microscopic observation. There are many examples of drug-induced formation of aberrant tubulin polymers that are either cold-stable or cold-labile.

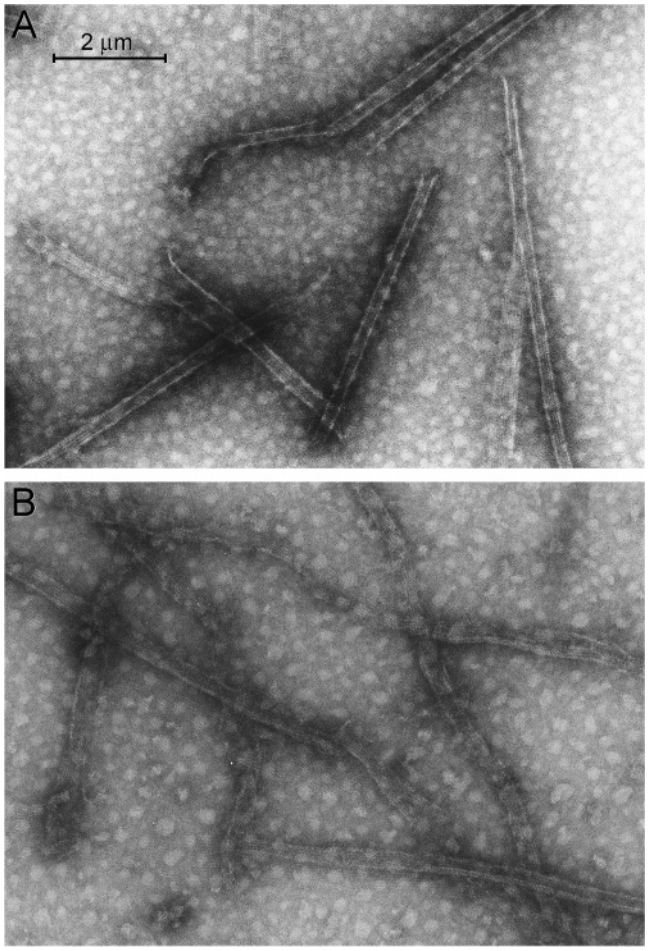

FIGURE 6: Electron micrographs of dictyostatin-induced polymer formed in the complete system (A) and in the tubulin-only system (B). The reaction mixtures were followed spectrophotometrically and prepared as described in Figure 5, with aliquots removed from the cuvettes either at the end of the 0 °C incubation (A) or the end of the 30 °C incubation (B).

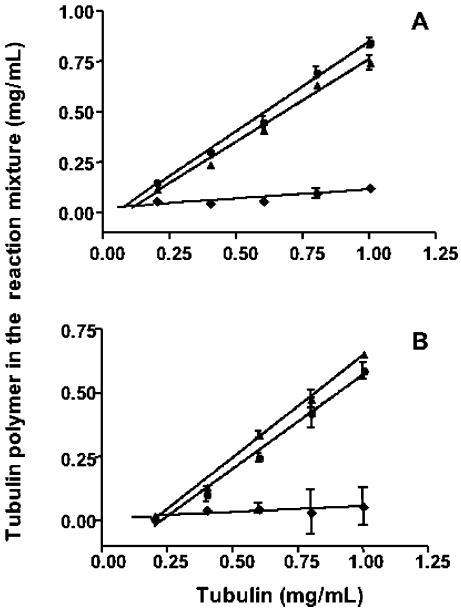

FIGURE 7: Tubulin critical concentration determinations with dictyostatin and discodermolide at 10 μM. (A) Complete system. (B) Tubulin-only system. In both panels: no test agent, diamonds; dictyostatin, circles; discodermolide, triangles. Reactions were carried out in 0.1 M Mes, pH 6.9, and the final concentration of DMSO in all cases was 4% v/v. Incubations were for 30 min at 37 °C followed by centrifugation for 15 min at 14 000 rpm at room temperature at 20−22 °C. An aliquot was removed from the supernatant and its protein concentration determined by the Lowry method. The critical concentration was the intersection of the interpolated control and test agent regression lines. The abscissa shows the concentrations of tubulin (mg/mL), while the ordinate values show the polymerized tubulin (mg/mL) present in the reaction mixture. Each data point was determined in triplicate. Critical concentration values in the complete system were 0.06 μM (0.006 mg/mL) for dictyostatin and 1.0 μM (0.1 mg/mL) for discodermolide. In the tubulin-only system, the critical tubulin concentrations were 2.5 μM (0.25 mg/mL) for dictyostatin and 2.1 μM (0.21 mg/mL) for discodermolide.

Many initial comparisons were made by electron microscopy of the various reaction conditions of dictyostatin-induced polymer with discodermolide-induced polymer and, when appropriate, paclitaxel-induced polymer. For any given reaction condition there was little overall difference in morphology of the polymer formed with any of the test agents in that microtubules and ribbon polymers were seen under all conditions. While relative proportions seemed to vary, this was difficult to quantitate. Two examples of dictyostatin-induced polymer are shown in Figure 6. Under both reaction conditions chosen, no polymer formed in the absence of test agent. Figure 6A shows the short MTs and ribbons, observed in the complete system after 1 h at 0 °C. Figure 6B shows the polymer, mostly in the form of short ribbons, observed in the tubulin-only system after 1 h at 30 °C.

Relative Quantitative Potencies of Dictyostatin and Discodermolide as Inducers of Tubulin Polymerization. The turbidimetry studies presented in Figures 4 and 5 indicated dictyostatin and discodermolide to have similar potencies as inducers of tubulin assembly. A more quantitative measurement of their relative activities was desired; to achieve this, two types of experiments were performed.

In the first set of experiments, tubulin critical concentrations were obtained using a centrifugation assay described previously (*34*) with the two test agents in the complete system (Figure 7A) and in the tubulin-only system (Figure 7B). The tubulin critical concentrations obtained were very similar for dictyostatin and discodermolide in each of the reaction conditions. In the complete system, the critical concentrations were 0.6 μM tubulin with dictyostatin and 1.0 μM tubulin with discodermolide. In the tubulin-only system, the values were 2.5 and 2.1 μM tubulin for dictyostatin and discodermolide, respectively. In the earlier study (*34*) in the tubulin-only system, tubulin critical concentration values of 1.5 and 5.9 μM were obtained for discodermolide and paclitaxel, respectively.

The second experimental approach was to determine for each test agent the concentration that would induce 50% assembly (EC_{50} value), as measured in a centrifugation assay (*35*). This assay exploits the interaction of MSG and tubulin in assembly reactions. In the absence of GTP, tubulin assembly will not occur in MSG unless a taxoidmimetic agent is present. In the case of paclitaxel, detailed studies show that the lower the MSG concentration the higher the EC_{50} value. Thus, the assay can be modulated to study taxoid site drugs both less active and more active than paclitaxel. In the studies summarized in Table 2, a low concentration of MSG (0.2 M) was used because of the potent activity of dictyostatin and discodermolide. Dictyostatin seemed slightly

Table 2: Concentrations of Dictyostatin, Discodermolide, and Paclitaxel Necessary To Cause 50% Assembly of a 10 μM Bovine Brain Tubulin Solution (EC_{50})

test agent	$EC_{50} \pm$ SD, μM (*N*)
dictyostatin	3.1 ± 0.2 (3)
discodermolide	3.6 ± 0.4 (3)
paclitaxel	25 ± 3 (3)

more active than discodermolide, with EC_{50} values for the two test agents of 3.1 and 3.6 μM, respectively, although the difference was within experimental error. Paclitaxel was much less active, with an EC_{50} value of 25 μM.

Effects of Dictyostatin on the Binding of [^{3}H]Paclitaxel, [^{14}C]Epothilone B, and [^{3}H]Discodermolide to Tubulin Polymer. Previous work shows that discodermolide strongly inhibits the binding of radiolabeled paclitaxel to tubulin polymer (*21*), while paclitaxel has little ability to inhibit the binding of radiolabeled discodermolide to polymer (*43*). Moreover, studies with radiolabeled paclitaxel at 37 °C have indicated the following order of affinity of taxoidmimetic drugs for the taxoid site: paclitaxel/epothilone A < docetaxel/epothilone B < discodermolide (*36*). More precise measurements of K_a values for the taxoids and epothilones, obtained by measuring inhibition of binding of a fluorescent taxoid to MTs (*44*), show the affinity of epothilone B to be significantly greater than the affinities of paclitaxel, docetaxel, and epothilone A (the K_a values at 37 °C for the four compounds were reported in ref *44* to be, respectively, 61, 1.1, 3.1, and 2.9 × 10^7 M^{-1}).

To confirm that dictyostatin bound to the taxoid site (*24*) and to obtain a preliminary idea of the relative affinity of dictyostatin for the site, its ability to inhibit the binding of [^{3}H]paclitaxel to tubulin polymer was examined and its activity compared to that of a number of other agents. The inhibitory effects of this group of agents on the binding of [^{14}C]epothilone B and [^{3}H]discodermolide were also examined. The results of experiments summarized in Table 3 demonstrate that dictyostatin was an effective inhibitor of the binding of all three radiolabeled ligands to tubulin polymer, and these experiments yielded data consistent with the relative affinities described above. This latter observation is clearest if the inhibitory effects of equimolar docetaxel or epothilone A are considered (in these experiments the concentration of each of the radiolabeled ligands was 4.0 μM). Epothilone A and docetaxel had negligible inhibitory effects on the binding of [^{3}H]discodermolide, intermediate effects on the binding of [^{14}C]epothilone B, and their greatest inhibitory effects on the binding of [^{3}H]paclitaxel to tubulin polymer.

Dictyostatin and discodermolide were nearly indistinguishable as inhibitors of paclitaxel and epothilone B binding. At first glance, it appears that the two agents are more effective as inhibitors of the binding of epothilone B (88−90% inhibition at equimolar concentrations) than of paclitaxel (76−77% inhibition at equimolar concentrations). However and for unknown reasons, the maximum inhibitory effect observed with the tritiated ligands (paclitaxel and discodermolide) was 70−80%, while over 90% inhibition of [^{14}C]-epothilone B binding was observed. The effects of lower concentrations of dictyostatin and discodermolide on paclitaxel and epothilone B binding were also examined, and again little difference was observed between the two compounds.

Table 3: Percent Inhibition by Test Agents of [^{3}H]Discodermolide, [^{14}C]Epothilone B, and [^{3}H]Paclitaxel Binding to Tubulin Polymer

	% inhibition + SD (*N*)		
inhibitor	[^{3}H]paclitaxel binding	[^{14}C]epothilone B binding	[^{3}H]discodermolide binding
discodermolide			
1 μM	61 ± 0.4 (3)	60 ± 6 (4)	nd[a]
2 μM	77 ± 1 (3)	84 ± 2 (4)	nd
4 μM	77 ± 5 (7)	90 ± 1 (3)	47 ± 6 (5)
50 μM	nd	93 ± 1 (3)	72 ± 8 (8)
dictyostatin			
1 μM	61 ± 2 (3)	55 ± 3 (4)	nd
2 μM	72 ± 3 (3)	77 ± 2 (4)	nd
4 μM	76 ± 4 (6)	88 ± 1 (3)	36 ± 5 (7)
20 μM	nd	nd	70 ± 1 (2)
epothilone B			
1 μM	53 ± 2 (3)	nd	nd
2 μM	64 ± 1 (3)	nd	nd
4 μM	71 ± 3 (7)	nd	14 ± 3 (3)
20 μM	nd	nd	31 ± 6 (2)
paclitaxel			
4 μM	nd	26 ± 1 (3)	6 ± 5 (3)
20 μM	nd	nd	3 ± 4 (2)
docetaxel			
4 μM	63 ± 8 (4)	36 ± 1 (3)	8 ± 6 (3)
epothilone A			
4 μM	53 ± 4 (4)	25 ± 3 (3)	6 ± 6 (3)

[a] Not determined.

When the inhibitory effects of dictyostatin on [^{3}H]-discodermolide binding were examined, the first impression was that dictyostatin bound somewhat less well than discodermolide, since only 36 ± 5% inhibition was observed with both compounds at 4.0 μM. However, a nearly identical effect (47 ± 6% inhibition) was obtained when 4.0 μM nonradiolabeled discodermolide was mixed with 4.0 μM [^{3}H]-discodermolide, reflecting the apparent inability to completely inhibit binding of the tritiated ligands to tubulin polymer noted above. This suggests that the affinities of dictyostatin and discodermolide for tubulin polymer are nearly identical. The only other test agent that showed significant ability to inhibit discodermolide binding at the concentrations examined was epothilone B. However, the inhibitory effect of 20 μM epothilone B was less than that of 4.0 μM dictyostatin or 4.0 μM nonradiolabeled discodermolide. This indicates that the affinity of dictyostatin and discodermolide for the taxoid site is at least 5-fold greater than that of epothilone B, assuming they have an identical or highly coincident binding site. Thus, it can be predicted, based on the work of Buey et al. (*44*), that the K_a value for dictyostatin and discodermolide will be greater than 3 × 10^9 M^{-1}.

DISCUSSION

The results of experiments using synthetic dictyostatin reported here show that, despite biochemical behavior almost indistinguishable from that of discodermolide and significantly greater than that of paclitaxel, the antiproliferative properties of the three drugs are not substantially different, confirming the observations of Isbrucker et al. with dictyostatin isolated from one of its natural sources (*20*). In addition, the present work extends their observation of retained antiproliferative activity in multidrug-resistant cells

to cells with mutations in the taxoid binding site that confer resistance to paclitaxel. Western blot and multiparameter cell-based fluorescence analyses showed that dictyostatin caused mitotic arrest and massive polymerization of cellular tubulin. Although implied by the earlier immunofluorescence work (*20*) and the characteristics of the interaction of dictyostatin with tubulin, these are important observations for adequate characterization of a tubulin interactive agent. Notably, in cells containing native tubulin (e.g., HeLa and 1A9), dictyostatin and paclitaxel were more active than were equimolar concentrations of discodermolide in inhibiting cell growth. In HeLa cells, the microtubule stabilizing activity as well as the ability to modulate cell cycle regulation and nuclear morphology, functions that likely contribute to growth inhibition and cytotoxicity, were consistently greater for paclitaxel and dictyostatin relative to the same concentration of discodermolide. In cells, dictyostatin had activity and potency similar to those of paclitaxel in modulating multiple cellular functions, despite being more structurally related to discodermolide.

The initial studies presented here of the inhibitory effects of dictyostatin and other agents on the binding of radiolabeled paclitaxel, epothilone B, and discodermolide to tubulin polymer confirm the conclusion from the assembly studies that dictyostatin binds avidly to tubulin polymer with an affinity little different from that of discodermolide. The current observations with the three radiolabeled ligands agree with earlier indications that discodermolide has particularly high affinity for the taxoid site (*21*, *43*). The present findings, when combined with the elegant quantitative analysis by Buey et al. (*44*) of taxoid and epothilone binding, indicate that the K_a values for the binding of dictyostatin and discodermolide to tubulin polymer will be greater than 3×10^9 M^{-1}. This conclusion is based on the reported K_a value for epothilone B of 6.1×10^8 M^{-1} (*44*) and the observation here that 20 μM epothilone B is less effective than 4 μM dictyostatin in inhibiting the binding of 4 μM dictyostatin to polymer.

While the inhibitory effects of dictyostatin have not yet been definitively evaluated, all studies to date with inhibitors of [^{3}H]paclitaxel binding to tubulin polymer have yielded competitive patterns: for epothilones A and B (*5*), for eleutherobin (*36*), and for discodermolide (*21*). Even though such a finding with discodermolide implies that it and paclitaxel bind at essentially the same site on tubulin polymer, cytotoxicity studies (*45*) have demonstrated synergism between the two agents that has not yet been demonstrated with other combinations of agents that bind at the taxoid site. Such synergism also appears to occur between discodermolide and paclitaxel when intracellular microtubule dynamics are examined (*46*), but no such synergy occurs in tubulin assembly reactions between paclitaxel, discodermolide, and dictyostatin (unpublished data). In contrast, assembly synergy can be readily demonstrated when laulimalide, which binds at a site on tubulin polymer distinct from the taxoid site (*47*), is combined with paclitaxel (*42*), or with discodermolide or dictyostatin (unpublished data). Perhaps a potential explanation for this puzzling discrepancy between the cytological and biochemical findings with discodermolide may lie in the recent report that discodermolide, but not paclitaxel, induces accelerated senescence in cells in culture (*48*).

The strikingly similar qualitative and quantitative results found in biochemical assays with dictyostatin and discodermolide strongly suggest that the bioactive conformation of discodermolide is mapped by that of dictyostatin, which matches the compact, tilde-shaped conformation present in the discodermolide X-ray crystal structure as well as the NMR structure determined in deuterated acetonitrile (*7*, *49*) versus the more open, extended structures suggested by the NMR analyses done with discodermolide dissolved in deuterated DMSO (*50*). Interestingly, dictyostatin was the more potent antiproliferative agent of the two, especially in HeLa cells. This could be due to several reasons, including the fact that the carbamate moiety on discodermolide, lacking from dictyostatin, is known to be labile but also necessary for biological activity (*51*), pointing to a potential cellular (or culture medium) solvolytic or metabolic instability of discodermolide. Alternatively, dictyostatin could simply enter cells more readily than discodermolide. All of these possibilities can be addressed in future studies. The results show that dictyostatin, although similar to discodermolide in several aspects, shows advantages in others and represents a good hit for drug discovery and lead for development. This is of consequence as the clinical development of discodermolide was recently halted (*52*).

ACKNOWLEDGMENT

The authors thank Drs. Kenneth Bair, Fred Kinder, and Markus Wartmann of Novartis for the generous gifts of discodermolide and epothilone B and their radiolabeled forms, Drs. Tito Fojo and Paraskevi Giannakakou for the 1A9 cells and their paclitaxel-resistant clones, and Profs. Simon Watkins and Donna Stolz and Ms. Ana Bursick of the University of Pittsburgh Center for Biological Imaging for their training in and assistance with electron microscopy.

REFERENCES

1. Schiff, P. B., Fant, J., Auste, L. A., and Horwitz, S. B. (1978) Effects of taxol on cell growth and in vitro microtubule assembly, *J. Supramol. Struct. 8*, Suppl. 2, 328.
2. Schiff, P. B., Fant, J., and Horwitz, S. B. (1979) Promotion of microtubule assembly in vitro by taxol, *Nature 277*, 665−667.
3. Gerth, K., Bedorf, N., Höfle, G., Irschik, H., and Reichenbach, H. J. (1996) Epothilons A and B: antifungal and cytotoxic compounds from *Sorangium cellulosum* (myxobacteria). Production, physico-chemical and biological properties, *J. Antibiot. 49*, 560−563.
4. Bollag, D. M., McQueney, P. A., Zhu, J., Hensens, O., Koupal, L., Liesch, J., Goetz, M., Lazarides, E., and Woods, C. M. (1995) Epothilones, a new class of microtubule-stabilizing agents with a Taxol-like mechanism of action, *Cancer Res. 55*, 2325−2333.
5. Kowalski, R. J., Giannakakou, P., and Hamel, E. (1997) Activities of the microtubule-stabilizing agents epothilones A and B with purified tubulin and in cells resistant to paclitaxel (Taxol®), *J. Biol. Chem. 272*, 2534−2541.
6. Altmann, K.-H., Wartmann, M., and O'Reilly, T. (2000) Epothilones and related structures—a new class of microtubule inhibitors with potent in vivo antitumor activity, *Biochim. Biophys. Acta 1470*, M79−M91.
7. Gunasekera, S. P., Gunasekera, M., Longley, R. E., and Schulte, G. K. (1990) Discodermolide: a new bioactive polyhydroxylated lactone from the marine sponge *Discodermia dissoluta*, *J. Org. Chem. 55*, 4912−4915; (correction) (1991) *J. Org. Chem. 56*, 1346.
8. ter Haar, E., Kowalski, R. J., Hamel, E., Lin, C. M., Longley, R. E., Gunasekera, S. P., Rosenkranz, H. S., and Day, B. W. (1996) Discodermolide, a cytotoxic marine agent that stabilizes microtubules more potently than taxol, *Biochemistry 35*, 243−250.

9. Quinoa, E., Kakou, Y., and Crews, P. (1988) Fijianolides, polyketide heterocyclics from a marine sponge, *J. Org. Chem. 53*, 3642−3644.
10. Corley, D. G., Herb, R., Moore, R. E., Scheuer, P. J., and Paul, V. J. (1988) Laulimalides: new potent cytotoxic macrolides from a marine sponge and a nudibranch predator, *J. Org. Chem. 53*, 3644−3646.
11. Mooberry, S. L., Tien, G., Hernandez, A. H., Plubrukarn, A., and Davidson, B. S. (1999) Laulimalide and isolaulimalide, new paclitaxel-like microtubule-stabilizing agents, *Cancer Res. 59*, 653−660.
12. Lindel, T., Jensen, P. R., Fenical, W., Long, B. H., Casazza, A. M., Carboni, J., and Fairchild, C. R. (1997) Eleutherobin, a new cytotoxin that mimics paclitaxel (Taxol) by stabilizing microtubules, *J. Am. Chem. Soc. 119*, 8744−8745.
13. Long, B. H., Carboni, J. M., Wasserman, A. J., Cornell, L. A., Casazza, A. M., Jensen, P. R., Lindel, T., Fenical, W., and Fairchild, C. R. (1998) Eleutherobin, a novel cytotoxic agent that induces tubulin polymerization, is similar to paclitaxel (Taxol), *Cancer Res. 58*, 1111−1115.
14. D'Ambrosio, M., Guerriero, A., and Pietra, F. (1987) Sarcodictyin A and sarcodictyin B, novel diterpenoidic alcohols esterified by (*E*)-*N*(1)-methylurocanic acid. Isolation from the Mediterranean stolonifer *Sarcodictyon roseum*, *Helv. Chim. Acta 70*, 2019−2027.
15. Ciomei, M., Albanese, C., Pastori, W., Grandi, M., Pietra, F., D'Ambrosio, M., Guerriero, A., and Battistini, C. (1997) Sarcodictyins: A new class of marine derivatives with mode of action similar to Taxol, *Proc. Am. Assoc. Cancer Res. 38*, 5.
16. West, L. M., Northcote, P. T., and Battershill, C. N. (2000) Peloruside A: a potent cytotoxic macrolide isolated from the New Zealand marine sponge *Mycale sp.*, *J. Org. Chem. 65*, 445−449.
17. Hood, K. A., West, L. M., Rouwe, B., Northcote, P. T., Berridge, M. V., Wakefield, S. J., and Miller, J. H. (2002) Peloruside A, a novel antimitotic agent with paclitaxel-like microtubule-stabilizing activity, *Cancer Res. 62*, 3356−3360.
18. Pettit, G. R., Cichacz, Z. A., Gao, F., Boyd, M. R., and Schmidt, J. M. (1994) Isolation and structure of the cancer cell growth inhibitor dictyostatin-1, *J. Chem. Soc., Chem. Commun. 9*, 1111−1112.
19. Shin, Y., Choy, N., Balachandran, R., Madiraju, C., Day, B. W., and Curran, D. P. (2002) Discodermolide/Dictyostatin hybrids: synthesis and biological evaluation, *Org. Lett. 4*, 4443−4446.
20. Isbrucker, R. A., Cummins, J., Pomponi, S. A., Longley, R. E., and Wright, A. E. (2003) Tubulin polymerizing activity of dictyostatin-1, a polyketide of marine sponge origin, *Biochem. Pharmacol. 66*, 75−82.
21. Kowalski, R. J., Giannakakou, P., Gunasekera, S. P., Longley, R. E., Day, B. W., and Hamel, E. (1997) The microtubule-stabilizing agent discodermolide competitively inhibits the binding of paclitaxel (Taxol) to tubulin polymers, enhances tubulin nucleation reactions more potently than paclitaxel, and inhibits the growth of paclitaxel-resistant cells, *Mol. Pharmacol. 52*, 613−622.
22. Paterson, I., Britton, R., Delgado, O., and Wright, A. E. (2004) Stereochemical determination of dictyostatin, a novel microtubule-stabilizing macrolide from the marine sponge *Corallistidae sp.*, *Chem. Commun. 6*, 632−633.
23. Shin, Y., Fournier, J. H., Fukui, Y., Brückner, A. M., and Curran, D. P. (2004) Total synthesis of (−)-dictyostatin: confirmation of relative and absolute configurations, *Angew. Chem., Int. Ed. 43*, 4634−4637.
24. Paterson, I., Britton, R., Delgado, O., Meyer, A., and Poullennec, K. G. (2004) Total synthesis and configurational assignment of (−)-dictyostatin, a microtubule-stabilizing macrolide of marine sponge origin, *Angew. Chem., Int. Ed. 43*, 4629−4633.
25. Hamel, E., and Lin, C. M. (1984) Separation of active tubulin and microtubule-associated proteins by ultracentrifugation and isolation of a component causing the formation of microtubule bundles, *Biochemistry 23*, 4173−4184.
26. Grover, S., and Hamel, E. (1994) The magnesium-GTP interaction in microtubule assembly, *Eur. J. Biochem. 222*, 163−172.
27. Wipf, P., Reeves, J. T., Balachandran, R., Giuliano, K. A., Hamel, E., and Day, B. W. (2000) Synthesis and biological evaluation of a focused mixture library of analogues of the antimitotic marine natural product curacin A, *J. Am. Chem. Soc. 122*, 9391−9395.
28. Lazo, J. S., Tamura, K., Vogt, A., Jung, J.-K., Rodriguez, S., Balachandran, R., Giuliano, K. A., Day, B. W., and Wipf, P. (2001) Antimitotic actions of a novel analog of the fungal metabolite palmarumycin CP1, *J. Pharmacol. Exp. Ther. 296*, 364−371.
29. Giannakakou, P., Sackett, D. L., Kang, Y. K., Zhan, Z., Buters, J. T., Fojo, T., and Poruchynsky, M. S. (1997) Paclitaxel-resistant human ovarian cancer cells have mutant beta-tubulins that exhibit impaired paclitaxel-driven polymerization, *J. Biol. Chem. 272*, 17118−17125.
30. Zhou, J., Gupta, K., Yao, J., Ye, K., Panda, D., Giannakakou, P., and Joshi, H. C. (2002) Paclitaxel-resistant human ovarian cancer cells undergo c-Jun NH2-terminal kinase-mediated apoptosis in response to noscapine, *J. Biol. Chem. 277*, 39777−39785.
31. Balachandran, R., Welsh, M. J., and Day, B. W. (2003) Altered levels and regulation of stathmin in paclitaxel-resistant ovarian cancer cells, *Oncogene 22*, 8924−8930.
32. Minguez, J. M., Balachandran, R., Madiraju, C., Giuliano, K. A., Curran, D. P., and Day, B. W. (2002) Synthesis and high content cell-based profiling of simplified analogues of the microtubule stabilizer (+)-discodermolide, *Mol. Cancer Ther. 1*, 1305−1313.
33. Giuliano, K. A., and Taylor, L. B. (1994) Fluorescent actin analogs with a high affinity for profilin in vitro exhibit an enhanced gradient of assembly in living cells, *J. Cell Biol. 124*, 971−983.
34. Dabydeen, D. A., Florence, G. J., Paterson, I., and Hamel, E. (2004) A quantitative evaluation of the effects of inhibitors of tubulin assembly on polymerization induced by discodermolide, epothilone B, and paclitaxel, *Cancer Chemother. Pharmacol. 53*, 397−403.
35. Lin, C. M., Jiang, Y. Q., Chaudhary, A. G., Rimoldi, J. M., Kingston, D. G. I., and Hamel, E. (1996) A convenient tubulin-based quantitative assay for paclitaxel (Taxol) derivatives more effective in inducing assembly than the parent compound, *Cancer Chemother. Pharmacol. 38*, 136−140.
36. Hamel, E., Sackett, D. C., Vourloumis, D., and Nicolaou, K. C. (1999) The coral-derived natural products eleutherobin and sarcodictyins A and B: effects on the assembly of purified tubulin with and without microtubule-associated proteins and binding at the polymer taxoid site, *Biochemistry 38*, 5490−5498.
37. Giuliano, K. A., Haskins, J. R., and Taylor, D. L. (2003) Advances in high content screening for drug discovery, *Assay Drug Dev. Technol. 1*, 565−577.
38. Abraham, V. C., Taylor, D. L., and Haskins, J. R. (2004) High content screening applied to large-scale cell biology, *Trends Biotechnol. 22*, 15−22.
39. Giuliano, K. A. (2003) High-content profiling of drug-drug interactions: cellular targets involved in the modulation of microtubule drug action by the antifungal ketoconazole, *J. Biomol. Screening 8*, 125−135.
40. Giuliano, K. A., Chen, Y. T., and Taylor, D. L. (2004) High-content screening with siRNA optimizes a cell biological approach to drug discovery: Defining the role of p53 activation in the cellular response to anticancer drugs, *J. Biomol. Screening 9*, 557−568.
41. Grover, S., Rimoldi, J. M., Molinero, A. A., Chaudhary, A. G., Kingston, D. G. I., and Hamel, E. (1995) Differential effects of paclitaxel (Taxol) analogs modified at positions C-2, C-7, and C-3′ on tubulin polymerization and polymer stabilization: identification of a hyperactive paclitaxel derivative, *Biochemistry 34*, 3927−3934.
42. Gapud, E. J., Bai, R., Ghosh, A. K., and Hamel, E. (2004) Laulimalide and paclitaxel: a comparison of their effects on tubulin assembly and their synergistic action when present simultaneously, *Mol. Pharmacol. 66*, 113−121.
43. Hung, D. T., Chen, J., and Schreiber, S. L. (1996) (+)-Discodermolide binds to microtubules in stoichiometric ratio to tubulin dimers, blocks taxol binding and results in mitotic arrest, *Chem. Biol. 3*, 287−293.
44. Buey, R. M., Díaz, J. F., Andreu, J. M., O'Brate, A., Giannakakou, P., Nicolaou, K. C., Sasmal, P. K., Ritzén, A., and Namoto, K. (2004) Interaction of epothilone analogs with the paclitaxel binding site: relationship between binding affinity, microtubule stabilization, and cytotoxicity, *Chem. Biol. 11*, 225−236.
45. Martello, L. A., McDaid, H. M., Regl, D. L., Yang, C. P., Meng, D., Pettus, T. R., Kaufman, M. D., Arimoto, H., Danishefsky, S. J., Smith, A. B., III, and Horwitz, S. B. (2000) Taxol and discodermolide represent a synergistic drug combination in human carcinoma cell lines, *Clin. Cancer Res. 6*, 1978−1987.
46. Honore, S., Kamath, K., Braguer, D., Horwitz, S. B., Wilson, L., Briand, C., and Jordan, M. A. (2004) Synergistic suppression of microtubule dynamics by discodermolide and paclitaxel in non-small cell lung carcinoma cells, *Cancer Res. 64*, 4957−4964.

47. Pryor, D. E., O'Brate, A., Bilcer, G., Díaz, J. F., Wang, Y., Wang, Y., Kabaki, M., Jung, M. K., Andreu, J. M., Ghosh, A. K., Giannakakou, P., and Hamel, E. (2002) The microtubule stabilizing agent laulimalide does not bind in the taxoid site, kills cells resistant to paclitaxel and epothilones, and may not require its epoxide moiety for activity, *Biochemistry 41*, 9109−9115.
48. Klein, L. E., Freeze, S., Smith, A. B., III, and Horwitz, S. B. (2005) The microtubule stabilizing agent discodermolide is a potent inducer of accelerated cell senescence, *Cell Cycle 4*, 501−507.
49. Smith, A. B., III, LaMarche, M. J., and Falcone-Hindley, M. (2001) Solution structure of (+)-discodermolide, *Org. Lett. 3*, 695−698.
50. Monteagudo, E., Cicero, D. O., Cornett, B., Myles, D. C., and Snyder, J. P. (2001) The conformations of discodermolide in DMSO, *J. Am. Chem. Soc. 123*, 6929−6930.
51. Hung, D. T., Nerenberg, J. B., and Schreiber, S. L. (1996) Syntheses of discodermolides useful for investigating microtubule binding and stabilization, *J. Am. Chem. Soc. 118*, 11054−11080.
52. Novartis, A. G. *Annual Report Pursuant to Section 13 or 15(d) of the Securities Exchange Act of 1934 for the fiscal year ended December 31, 2004*, Securities Exchange Commission file number 1-15024, Form 20-F, filed Jan 28, 2005, p 42.

BI050685L